Spatial control of membrane receptor function using ligand nanocalipers

Alan Shaw[1,4], Vanessa Lundin[2,4], Ekaterina Petrova[2], Ferenc Fördős[1], Erik Benson[1], Abdullah Al-Amin[2], Anna Herland[2], Andries Blokzijl[3], Björn Högberg[1,5] & Ana I Teixeira[2,5]

The spatial organization of membrane-bound ligands is thought to regulate receptor-mediated signaling. However, direct regulation of receptor function by nanoscale distribution of ligands has not yet been demonstrated, to our knowledge. We developed rationally designed DNA origami nanostructures modified with ligands at well-defined positions. Using these 'nanocalipers' to present ephrin ligands, we showed that the nanoscale spacing of ephrin-A5 directs the levels of EphA2 receptor activation in human breast cancer cells. Furthermore, we found that the nanoscale distribution of ephrin-A5 regulates the invasive properties of breast cancer cells. Our ligand nanocaliper approach has the potential to provide insight into the roles of ligand nanoscale spatial distribution in membrane receptor–mediated signaling.

Cells that are nearest neighbors coordinate their activities in tissues through interactions between membrane-bound receptors that specifically bind ligands presented by adjacent cells. This coordination is often dysregulated in cancer, allowing cells to acquire abnormal functions such as aberrant proliferation and invasion of neighboring tissues. The nanoscale distribution of ligands is hypothesized to regulate signaling mediated by membrane receptors, whereby subtle differences in ligand nanoarchitecture are translated into a diversity of cellular responses[1]. However, the underlying mechanisms are poorly understood owing to difficulties in controlling the spatial distribution of protein assemblies at the nanoscale. Previous approaches for studies of ligand and receptor clustering have used either patterning of surface-anchored ligands[2,3] or antibody-mediated clustering in solution[4]. In contrast, the approach we present utilizes DNA nanotechnology to control the spatial distribution of ligands and offers accurate nanoscale distance manipulation, which can be tuned independently of ligand concentration. This tool, which we call ligand nanocalipers, produces precise patterns of ligands, enabling us to map the relationships between the nanoscale spacing of ligands and receptor activation, intracellular signaling and cellular outcomes. Further, nanocalipers display the ligands in solution phase, similarly to the antibody clustering method, a characteristic allowing nanocalipers to be added to the medium of cells cultured in standard conditions. The method can therefore be used to manipulate cells in three-dimensional tissue models and, as such, has the potential to provide new knowledge for development of therapeutic strategies.

We applied our ligand nanocaliper method to investigate the roles of the spatial distribution of ephrin ligands in Eph receptor function. Eph receptors bind ephrins in adjacent cells, inducing receptor phosphorylation and activation of intracellular signaling pathways that primarily regulate cell migration and proliferation. Eph receptor signaling is critical in many developmental processes and is frequently disrupted in cancer, showing either tumor-promoting or tumor-suppressing effects, depending on the cellular microenvironment[5–8]. Mounting evidence suggests that the nanoscale spatial distribution of ephrin ligands is a relevant physical signal in Eph receptor activation[1,2,9], potentially contributing to the diversity of cell outcomes. For example, soluble recombinant ephrin dimers induce Eph receptor phosphorylation to a larger extent than monomers[10,11], which reflects the receptor dimerization requirement for the release of kinase-domain autoinhibition. Moreover, higher-order clusters of recombinant ephrins in solution, produced by combining ephrin-Fc fusion proteins with anti-Fc antibodies, have been found to produce a subset of cellular responses *in vitro*, such as the formation of endothelial tubes, which are not elicited by ephrin dimers[12]. Interestingly, constraining the lateral mobility of ephrin-A1 ligands in supported lipid bilayers causes spatial reorganization of EphA2 receptors and modulates cytoskeletal morphology in overlying cells[2]. *In vivo*, EphA4 has been shown to have higher-order cluster-dependent functions in neurodevelopment, such as hindlimb locomotion, as well as cluster-independent activities[13]. Using ligand nanocalipers, we showed that the nanoscale spatial distribution of ephrin-A5 ligands tunes EphA2 receptor activation levels and the invasive properties of breast cancer cells.

RESULTS

Design and synthesis of ephrin-A5 nanocalipers

To investigate the roles of ligand nanoscale spacing in EphA2 receptor activation, we developed a collection of nanostructures, with each set of structures displaying ephrin-A5 ligands at a

[1]Swedish Medical Nanoscience Center, Department of Neuroscience, Karolinska Institutet, Stockholm, Sweden. [2]Department of Cell and Molecular Biology, Karolinska Institutet, Stockholm, Sweden. [3]Department of Immunology, Genetics and Pathology, Uppsala University, Uppsala, Sweden. [4]These authors contributed equally to this work. [5]These authors jointly directed this work. Correspondence should be addressed to A.I.T. (ana.teixeira@ki.se) or B.H. (bjorn.hogberg@ki.se).

RECEIVED 8 JULY 2013; ACCEPTED 20 MAY 2014; PUBLISHED ONLINE 6 JULY 2014; DOI:10.1038/NMETH.3025

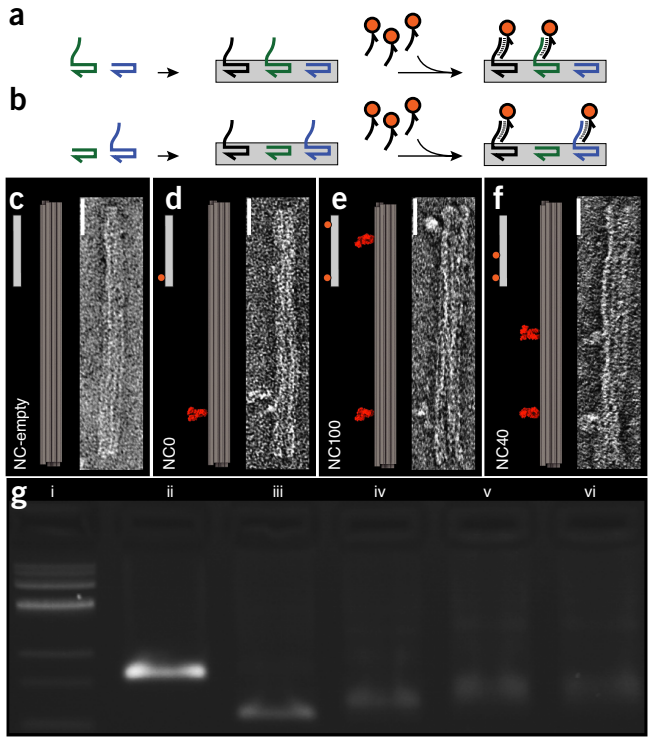

Figure 1 | The nanocaliper principle and display of ephrin ligands. (**a**,**b**) By slightly varying the DNA oligonucleotide sequences (as depicted by different colors) used for assembling a DNA origami nanocaliper, protruding 5′ ssDNA handles can be placed in different positions. Using a protruding version of the black and green sequences, or protruding versions of the black and blue sequences, leaves binding sites at different positions for protein ligands (orange circles) conjugated to the 3′ ends of a DNA oligonucleotide bearing a common complementary binding sequence (black strands). (**c**–**f**) TEM micrographs of 18-helix bundle DNA origami nanotube nanocalipers. The nanostructures were prepared without protein binding sites (NC-empty; **c**), with one binding site (NC0; **d**) or with two binding sites 101.1 nm apart (NC100; **e**) or 42.9 nm apart (NC40; **f**). Scale bars, 20 nm. (**g**) 2% agarose gel run with a 1-kb DNA ladder (i), p7560 ssDNA (ii), NC-empty (iii), NC0 (iv), NC100 (v) and NC40 (vi) and stained with ethidium bromide.

different distance. These solution-phase ligand nanocalipers bound EphA2 receptors and were able to move laterally on the cell membrane. We achieved this using DNA nanotechnology[14,15], which has recently showed increasing promise for nanoscale positioning of proteins[16–22]. By using DNA origami methods[15,23,24], we designed a base nanocaliper structure and then modified it to display short ssDNA sequences at the surface at regular intervals. Ephrin-A5-Fc chimeric protein, which spontaneously forms ephrin-A5 dimers, was conjugated to the 3′ end of a target ssDNA oligonucleotide (**Supplementary Fig. 1**) that was designed to hybridize to the sequences displayed at the surface of the nanocalipers (**Fig. 1a**,**b**). These ephrin-A5-Fc–oligonucleotide conjugates are henceforth referred to as ephrin-A5 conjugates.

The base design for our nanocalipers was a DNA origami structure comprising 18 parallel double helices in a hollow tube-like arrangement (**Supplementary Fig. 2** and **Supplementary Table 1**). We modified this base design (NC-empty; **Fig. 1c**) to display protruding 5′ ssDNA handles to bind ephrin-A5 conjugates through hybridization (**Supplementary Fig. 3**). Each binding site was implemented as a pair of protruding ends separated by three double helices in a honeycomb arrangement[23] to ensure a high yield of bound ephrin-A5 conjugates at each site. The binding sites were separated along the helical direction by 100.1 nm or 42.9 nm, conditions hereafter referred to as NC100 (**Fig. 1e**) and NC40 (**Fig. 1f**), respectively. Further, we generated two nanostructures, one with a single binding site, NC0 (**Fig. 1d**), and the other, NC-sat, with a saturated amount of protruding ends (i.e., using all available binding sites in the design), resulting in eight binding sites separated by 14.3 nm (**Supplementary Figs. 2**–**4**). Membrane microdomains with dimensions ranging from 10 to 200 nm are thought to mediate spatial regulation of receptor signaling[3,25,26]. Therefore, we designed our tool to control spatial distributions of ligands within this range. The 100-nm spacing is approximately the limit of what can be achieved with a rigid DNA origami using the currently available scaffolds, and the 43-nm spacing was selected as an intermediate distance. The DNA origami structures were folded as described elsewhere[15,23,27].

Characterization of ephrin-A5 nanocalipers

We verified the successful fabrication of the ephrin-A5 nanocalipers by transmission electron microscopy (TEM) (**Fig. 1c**–**f** and **Supplementary Fig. 4**). In addition to TEM, agarose gel shift assays confirmed efficient hybridization of the ephrin-A5 conjugates to the nanocalipers, indicating that the fractions of NC100 and NC40 bound with two dimers were close to 90% (**Fig. 1g** and **Supplementary Figs. 5**–**8**).

To analyze the binding ability of the ephrin-A5 conjugates and complete ephrin-A5 nanocalipers to the EphA2 receptor, we performed surface plasmon resonance (SPR) measurements. The binding of the ephrin-A5 conjugates to the extracellular domain of human EphA2 was compared to that of the unmodified ephrin-A5-Fc (**Supplementary Fig. 9**). The measurements showed no clear loss of binding activity upon conjugation of the ligand, which indicates that the bioavailability of ephrin-A5 was retained. This is in line with our estimate that more than 95% of the binding domains of ephrin-A5 are available for EphA2 binding after conjugation (**Supplementary Fig. 10**). Further, we performed SPR analysis on ephrin-A5 nanocalipers (**Fig. 2a** and **Supplementary Figs. 9** and **11**), and the results showed that NC0 exhibited similar binding affinity to that of unmodified ephrin-A5-Fc and ephrin-A5 conjugates, indicating that conjugation and further hybridization to the nanocalipers does not interfere with the ephrin-A5 binding activity. Moreover, NC100 and NC40 showed an enhancement in EphA2 binding affinity compared to NC0, indicating that NC100 and NC40 are able to bind EphA2 with avidity. To complement the SPR binding assay, we performed a magnetic bead–based EphA2 pulldown assay with the ephrin-A5 nanocalipers (**Supplementary Fig. 12**) to probe the amount of ephrin-A5 on the nanocalipers available for EphA2 binding. The results showed clear EphA2 binding activity that scaled well with the designed number of binding sites on the nanocalipers, and, notably, NC100 and NC40 showed similar binding. Together, the results from the TEM imaging, gel shift assays, SPR binding and EphA2 pulldown assay support the conclusion that the ephrin-A5 nanocalipers are produced with the anticipated stoichiometry of biological active ligands.

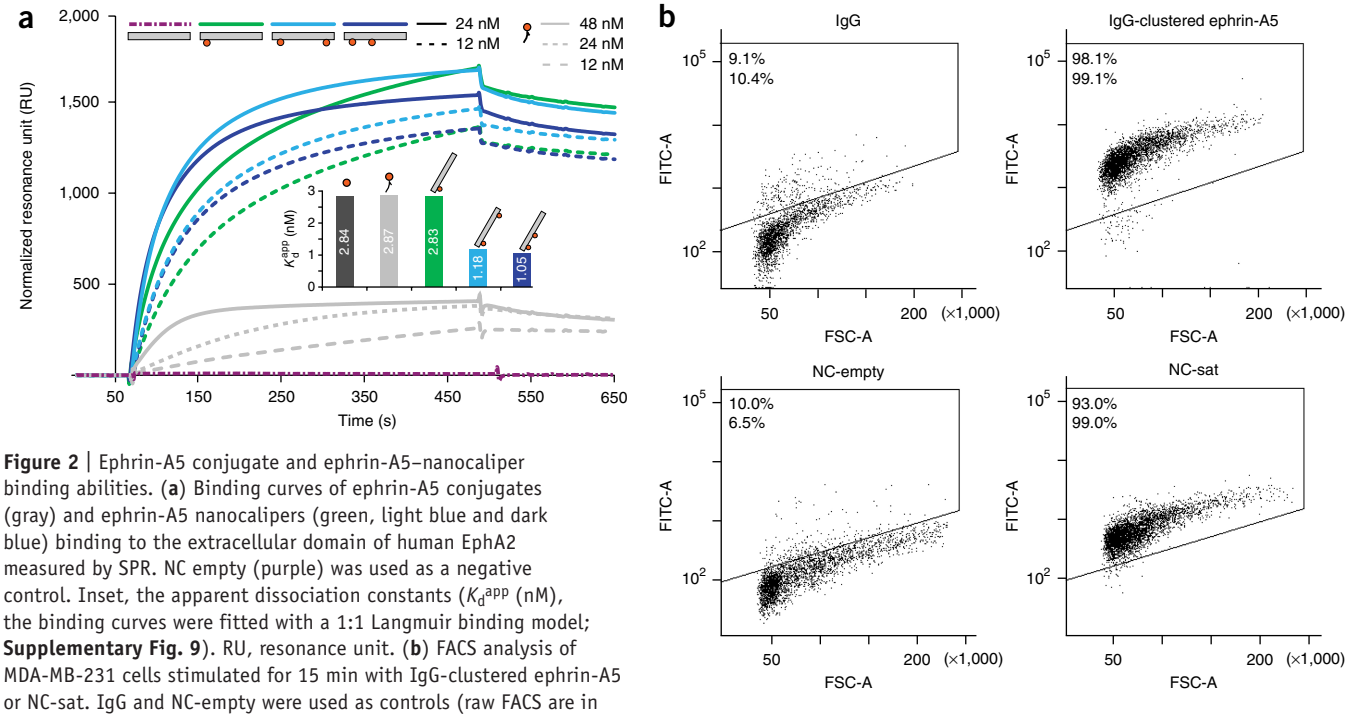

Figure 2 | Ephrin-A5 conjugate and ephrin-A5–nanocaliper binding abilities. (**a**) Binding curves of ephrin-A5 conjugates (gray) and ephrin-A5 nanocalipers (green, light blue and dark blue) binding to the extracellular domain of human EphA2 measured by SPR. NC empty (purple) was used as a negative control. Inset, the apparent dissociation constants (K_d^{app} (nM), the binding curves were fitted with a 1:1 Langmuir binding model; **Supplementary Fig. 9**). RU, resonance unit. (**b**) FACS analysis of MDA-MB-231 cells stimulated for 15 min with IgG-clustered ephrin-A5 or NC-sat. IgG and NC-empty were used as controls (raw FACS are in the **Supplementary Data**). DyLight 488-conjugated anti-human IgG was used to precluster the ephrin-A5 for 15 min. DyLight 488–conjugated anti-human IgG was added to the cell culture medium 15 min after EphA2 stimulation with NC-sat and NC-empty. The percentage of fluorescently labeled cells is indicated in the plots, calculated as average ± s.e.m. from 2 independent biological repeats. FSC-A, forward scatter; FITC-A, fluorescein isothiocyanate.

To investigate whether ephrin-A5 nanocalipers were capable of binding EphA2 in an MDA-MB-231 human breast cancer cell line, we performed FACS analysis (**Fig. 2b** and **Supplementary Data**). NC-sat showed extensive binding to cells, whereas NC-empty showed minimal binding. Similarly, IgG-clustered ephrin-A5 showed increased binding to cells compared to that observed with IgG. Thus, ephrin-A5 nanocalipers efficiently bind to EphA2-expressing cells.

Ephrin-A5 nanocalipers direct EphA2 phosphorylation

To quantify EphA2 receptor phosphorylation, we used an *in situ* proximity ligation assay (PLA)[28]. To enable accurate quantification, we cultured MDA-MB-231 cells as single cells on substrates with micropatterned fibronectin islands of defined size, which prevent receptor activation through cell-cell contact, resulting in a PLA that is highly sensitive and reproducible. We first

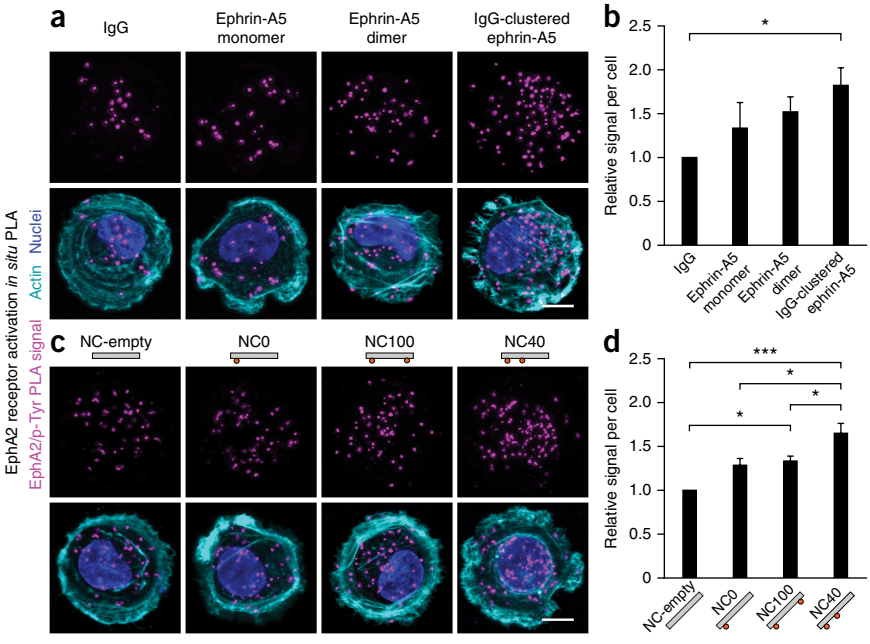

Figure 3 | The spatial distribution of ephrin-A5 ligands directs the phosphorylation levels of the EphA2 receptor. (**a**) Phosphorylation of the EphA2 receptor (EphA2/p-Tyr) in MDA-MB-231 cells cultured on fibronectin micropatterns after 15 min of treatment with IgG, ephrin-A5 monomer, ephrin-A5 dimer or IgG-clustered ephrin-A5, detected with PLA (purple dots). (**b**) Quantification of the PLA of phosphorylated EphA2 receptor (averages). Error bars, s.e.m.; $n = 7$ biological replicates for all conditions except monomer, where $n = 5$. (**c**) Phosphorylated EphA2 receptor (purple dots) in MDA-MB-231 cells cultured on fibronectin micropatterns, detected by PLA. Cells were treated with NC-empty, NC0, NC100 or NC40 for 15 min. (**d**) Quantification of the PLA of phosphorylated EphA2 receptor in MDA-MB-231 cells grown on fibronectin micropatterns (averages). Error bars, s.e.m.; $n = 6$ biological replicates for all conditions except NC0, where $n = 4$. One-way analysis of variance (ANOVA) was used followed by Tukey's multiple-comparison test. Cells in **a** and **c** were stained for the actin cytoskeleton using Alexa 488–phalloidin (turquoise), and the nuclei using DAPI (blue). In all cases, PLA signal quantification was performed on >20 cells for each condition, for each biological repeat (*$P < 0.05$, ***$P < 0.001$). Scale bars, 10 µm.

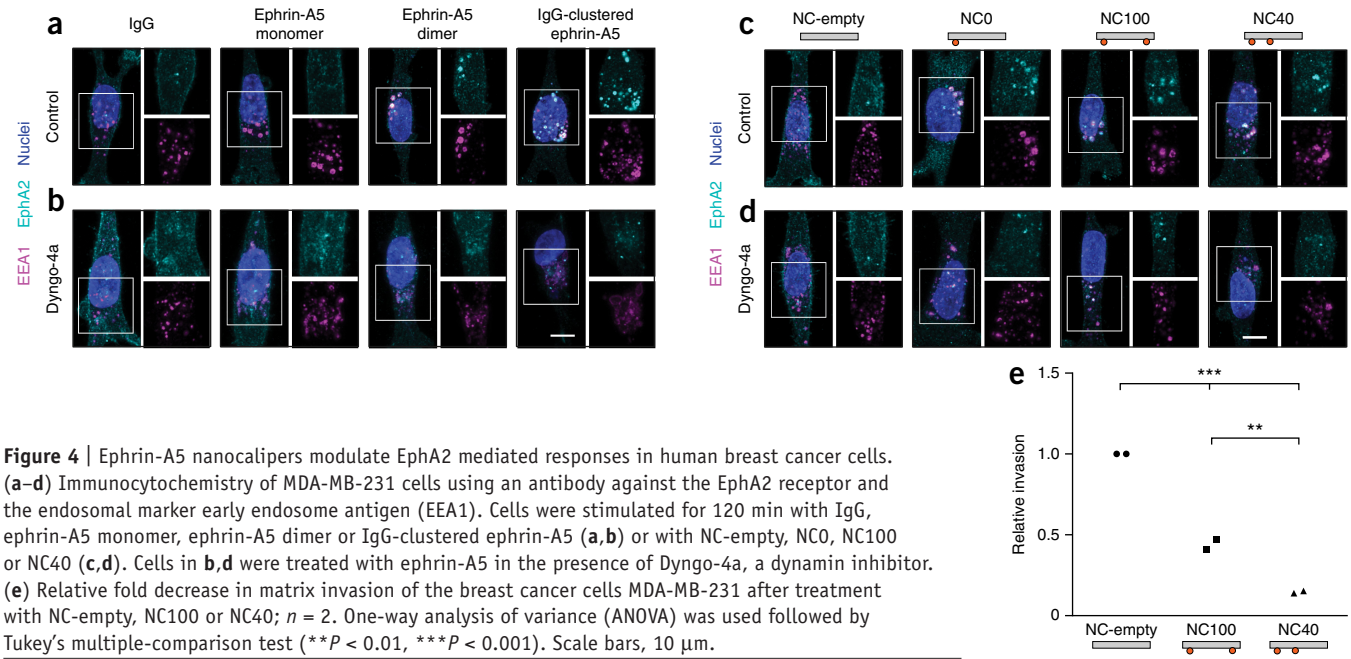

Figure 4 | Ephrin-A5 nanocalipers modulate EphA2 mediated responses in human breast cancer cells. (**a**–**d**) Immunocytochemistry of MDA-MB-231 cells using an antibody against the EphA2 receptor and the endosomal marker early endosome antigen (EEA1). Cells were stimulated for 120 min with IgG, ephrin-A5 monomer, ephrin-A5 dimer or IgG-clustered ephrin-A5 (**a**,**b**) or with NC-empty, NC0, NC100 or NC40 (**c**,**d**). Cells in **b**,**d** were treated with ephrin-A5 in the presence of Dyngo-4a, a dynamin inhibitor. (**e**) Relative fold decrease in matrix invasion of the breast cancer cells MDA-MB-231 after treatment with NC-empty, NC100 or NC40; $n = 2$. One-way analysis of variance (ANOVA) was used followed by Tukey's multiple-comparison test ($^{**}P < 0.01$, $^{***}P < 0.001$). Scale bars, 10 μm.

analyzed the phosphorylation of the EphA2 receptor in response to commonly used conditions to study Eph receptor signaling using recombinant ligands (using 10 nM of ephrin-A5-Fc). We observed the predicted gradual increase in receptor phosphorylation in cells treated with IgG, ephrin-A5 monomers, ephrin-A5 dimers (ephrin-A5-Fc) and IgG-clustered ephrin-A5-Fc (**Fig. 3a**,**b** and **Supplementary Fig. 13**). EphA2 immunoprecipitations followed by anti-phosphotyrosine immunoblotting of cells treated with IgG, ephrin-A5 monomer, ephrin-A5 dimer and IgG-clustered ephrin-A5 showed similar activation trends to those seen with the PLA (**Supplementary Fig. 14**). Immunoprecipitation of cells treated with NC-empty, NC0, NC100 and NC40 showed that ephrin-A5 nanocalipers induced receptor phosphorylation at levels comparable to those triggered by ephrin-A5 dimers and IgG-clustered ephrin-A5 (**Supplementary Fig. 14**).

We next quantified receptor phosphorylation induced by ephrin-A5 nanocalipers using a PLA. All ephrin-A5 nanocalipers (using 10 nM total concentration of ephrin-A5-Fc), NC0, NC100 and NC40 induced receptor phosphorylation compared to the NC-empty control. NC0, which contains a single ephrin-A5 dimer, showed similar activation levels of EphA2 to those of NC100, at equivalent molar amounts of ephrin-A5, suggesting that no proximity effects are observed in EphA2 phosphorylation induced by NC100. Interestingly, NC40 was more efficient at inducing EphA2 receptor phosphorylation than NC100 (**Fig. 3c**,**d**). Our conclusion that this effect is due to proximity and not differences in binding is strengthened by the fact that the NC100 and NC40 showed similar binding affinity in SPR (**Fig. 2a**) and similar binding stoichiometry in the EphA2 pulldown assay (**Supplementary Fig. 12**).

To investigate the effects of local stoichiometry on the activation of EphA2 receptor, we compared the phosphorylation levels induced by NC40 and NC-sat. Interestingly, though NC-sat had an increased local stoichiometry of ephrin-A5 dimers, we observed no increase in the levels of phosphorylated EphA2 receptors detected by PLA (**Supplementary Fig. 15**). Together, these results indicate that the nanoscale spatial distribution of ephrin-A5 tunes the levels of activated EphA2 receptors.

Nanocalipers induce dynamin-dependent EphA2 endocytosis

Activation of Eph receptors is followed by endocytosis, leading to termination of the signal[29,30]. To investigate the endocytosis of EphA2 in response to ephrin-A5 nanocalipers, we performed immunocytochemistry experiments of EphA2 receptor and early endosome antigen 1 (EEA1) upon treatment with NC-empty, NC0, NC100 and NC40. The results showed EphA2 receptor internalization and translocation to early endosomes after 2 h of stimulation with ephrin-A5 nanocalipers, similarly to cells treated with ephrin-A5 dimers or IgG-clustered ephrin-A5 (**Fig. 4a**,**c**). In contrast, treatment with NC-empty, IgG or ephrin-A5 monomer did not cause detectable receptor endocytosis during this time (**Fig. 4a**,**c**). These results suggest that there is endocytosis of EphA2 following activation upon treatment with ephrin-A5 nanocalipers. Moreover, to investigate the mechanisms of endocytosis following receptor activation, we inhibited endocytosis using a dynamin inhibitor, Dyngo-4a. Dynamin inhibition hampered EphA2 endocytosis in ephrin-A5 nanocaliper–treated cells, similarly to cells treated with ephrin-A5 dimer or IgG-clustered ephrin-A5 (**Fig. 4b**,**d**). Therefore, EphA2 endocytosis following ephrin-A5–nanocaliper stimulation is, at least partially, mediated by dynamin.

Ephrin-A5 nanocalipers modulate cell invasion

The EphA2 receptor is overexpressed in many cancers, and high expression levels generally correlate with poor prognosis[5]. EphA2 is often weakly phosphorylated in tumors and engages in ligand-independent signaling that promotes cell invasion[6,31]. Receptor activation, using recombinant ligands or activating antibodies, inhibits cell proliferation and migration and shows tumor-suppressive effects[32]. Accordingly, IgG-clustered ephrin-A5 caused a decrease in cell invasion compared to IgG alone (**Supplementary Fig. 16**). EphA2 activation in MDA-MB-231 cells

by ephrin-A5 nanocalipers significantly decreased cell invasiveness compared to cells treated with empty nanocalipers (**Fig. 4e**). Notably, NC40 caused a larger decrease in cell migration than NC100. This is in line with the higher activation of EphA2 receptor by NC40 compared to NC100 (**Fig. 3d**). In conclusion, ephrin-A5 nanocalipers appear capable of modulating suppression of migration by the activated EphA2 receptor.

DISCUSSION

We have developed a method to efficiently present ligands to cell membrane–bound receptors with tailor-made nanoscale spatial distributions using DNA origami nanofabrication. Our ligand nanocalipers offer the opportunity to investigate the roles of nanoscale spatial distribution of ligands on receptor activation and cellular responses in a solution-phase display. Here, we used this method to demonstrate that the levels of phosphorylation of the EphA2 receptor are controlled by the nanoscale distribution of ephrin-A5 ligands. Analysis of the crystal structure of EphA2 associated with ephrin-A5 gave rise to the hypothesis that ligand-receptor binding is followed by recruitment of non-ligand-bound EphA2 in a seeding mechanism[33–35]. Our results suggest that NC40 is more efficient at triggering this effect than NC100. Moreover, NC-sat did not further increase the activation levels compared to NC40. This suggests that the decrease in spacing of ephrin-A5 in NC-sat, and increase in local stoichiometry, does not induce more efficient seeding of EphA2 clusters. Interestingly, NC0, which contains a single ephrin-A5 dimer, showed similar activation levels of EphA2 to those of NC100. This points to a loss of proximity effects in EphA2 activation for NC100. Together, these results show that EphA2 receptor activation is sensitive to the initial ephrin-A5 spatial distribution upon binding. Furthermore, we showed that the nanoscale spatial distribution of ephrin-A5 tunes the invasive properties of breast cancer cells.

Ligand nanocalipers can control the spatial organization of signaling at the cell membrane, which in turn tunes receptor activity and cellular outcomes. This may potentially be relevant in targeting Eph-mediated signaling, which can simultaneously activate tumor-promoting and tumor-suppressing signaling pathways[8]. We suggest that this method could be used to address the roles of nanoscale distribution of ligands in other signaling pathways regulating cell-cell communication. The knowledge gained from such studies has the potential to provide new insights relevant for the development of pharmacological interventions that target the biophysical context of the ligand-receptor interaction.

METHODS

Methods and any associated references are available in the online version of the paper.

Note: Any Supplementary Information and Source Data files are available in the online version of the paper.

ACKNOWLEDGMENTS

We thank U. Lendahl and his lab (Karolinska Institutet) for reagents and discussions, J. Avila-Cariño for help with the FACS experiments, O. Shupliakov for help with TEM, G. Bernardinelli for help with rendering ephrin-A5 and Y.-X. Zhao for help with initial experiments. This work was funded through grants from the Swedish Research Council to B.H. (repatriation grant 2010-6296 and project grant 2010-5060) and by the Strategic Research Program in Stem Cell Research and Regenerative Medicine at Karolinska Institutet (StratRegen), Sweden (A.I.T.). B.H. received startup funding from Carl Bennet AB, Karolinska Institutet and the Swedish Governmental Agency for Innovation Systems (Vinnova). V.L. and A.S. were supported by KID doctoral fellowships from the Karolinska Institutet, Sweden.

AUTHOR CONTRIBUTIONS

B.H. and A.I.T. conceived of and designed the study. V.L., A.S. and E.P. performed most of the experimental work. F.F. and E.B. contributed to nanostructure and conjugate production and nanocaliper characterization. A.A.-A., A.H. and A.B. contributed to cell culture and the setting up and validating of the PLA assay. A.B. performed immunoprecipitation and immunoblotting experiments. V.L., A.S., B.H. and A.I.T. wrote the manuscript. All authors contributed to manuscript proofing and discussion.

COMPETING FINANCIAL INTERESTS

The authors declare no competing financial interests.

1. Casaletto, J.B. & McClatchey, A.I. Spatial regulation of receptor tyrosine kinases in development and cancer. *Nat. Rev. Cancer* **12**, 387–400 (2012).
2. Salaita, K. *et al.* Restriction of receptor movement alters cellular response: physical force sensing by EphA2. *Science* **327**, 1380–1385 (2010).
3. Lohmüller, T. *et al.* Supported membranes embedded with fixed arrays of gold nanoparticles. *Nano Lett.* **11**, 4912–4918 (2011).
4. Holmberg, J. *et al.* Ephrin-A2 reverse signaling negatively regulates neural progenitor proliferation and neurogenesis. *Genes Dev.* **19**, 462–471 (2005).
5. Pasquale, E.B. Eph receptors and ephrins in cancer: bidirectional signalling and beyond. *Nat. Rev. Cancer* **10**, 165–180 (2010).
6. Miao, H. *et al.* EphA2 mediates ligand-dependent inhibition and ligand-independent promotion of cell migration and invasion via a reciprocal regulatory loop with Akt. *Cancer Cell* **16**, 9–20 (2009).
7. Batlle, E. *et al.* EphB receptor activity suppresses colorectal cancer progression. *Nature* **435**, 1126–1130 (2005).
8. Genander, M. *et al.* Dissociation of EphB2 signaling pathways mediating progenitor cell proliferation and tumor suppression. *Cell* **139**, 679–692 (2009).
9. Bethani, I., Skånland, S.S., Dikic, I. & Acker-Palmer, A. Spatial organization of transmembrane receptor signalling. *EMBO J.* **29**, 2677–2688 (2010).
10. Davis, S. *et al.* Ligands for EPH-related receptor tyrosine kinases that require membrane attachment or clustering for activity. *Science* **266**, 816–819 (1994).
11. Wykosky, J. *et al.* Soluble monomeric EphrinA1 is released from tumor cells and is a functional ligand for the EphA2 receptor. *Oncogene* **27**, 7260–7273 (2008).
12. Stein, E. *et al.* Eph receptors discriminate specific ligand oligomers to determine alternative signaling complexes, attachment, and assembly responses. *Genes Dev.* **12**, 667–678 (1998).
13. Egea, J. *et al.* Regulation of EphA 4 kinase activity is required for a subset of axon guidance decisions suggesting a key role for receptor clustering in Eph function. *Neuron* **47**, 515–528 (2005).
14. Seeman, N.C. Nanomaterials based on DNA. *Annu. Rev. Biochem.* **79**, 65–87 (2010).
15. Rothemund, P.W.K. Folding DNA to create nanoscale shapes and patterns. *Nature* **440**, 297–302 (2006).
16. Högberg, B. & Olin, H. DNA-scaffolded nanoparticle structures. *J. Phys. Conf. Ser.* **61**, 458–462 (2007).
17. Voigt, N.V. *et al.* Single-molecule chemical reactions on DNA origami. *Nat. Nanotechnol.* **5**, 200–203 (2010).
18. Selmi, D.N. *et al.* DNA-templated protein arrays for single-molecule imaging. *Nano Lett.* **11**, 657–660 (2011).
19. Rinker, S., Ke, Y., Liu, Y., Chhabra, R. & Yan, H. Self-assembled DNA nanostructures for distance-dependent multivalent ligand-protein binding. *Nat. Nanotechnol.* **3**, 418–422 (2008).
20. Park, S.H. *et al.* Programmable DNA self-assemblies for nanoscale organization of ligands and proteins. *Nano Lett.* **5**, 729–733 (2005).
21. Derr, N.D. *et al.* Tug-of-war in motor protein ensembles revealed with a programmable DNA origami scaffold. *Science* **338**, 662–665 (2012).
22. Douglas, S.M., Bachelet, I. & Church, G.M. A logic-gated nanorobot for targeted transport of molecular payloads. *Science* **335**, 831–834 (2012).

23. Douglas, S.M. *et al.* Self-assembly of DNA into nanoscale three-dimensional shapes. *Nature* **459**, 414–418 (2009).
24. Andersen, E.S. *et al.* Self-assembly of a nanoscale DNA box with a controllable lid. *Nature* **459**, 73–76 (2009).
25. Abulrob, A. *et al.* Nanoscale imaging of epidermal growth factor receptor clustering: effects of inhibitors. *J. Biol. Chem.* **285**, 3145–3156 (2010).
26. Lajoie, P. *et al.* Plasma membrane domain organization regulates EGFR signaling in tumor cells. *J. Cell Biol.* **179**, 341–356 (2007).
27. Castro, C.E. *et al.* A primer to scaffolded DNA origami. *Nat. Methods* **8**, 221–229 (2011).
28. Söderberg, O. *et al.* Direct observation of individual endogenous protein complexes *in situ* by proximity ligation. *Nat. Methods* **3**, 995–1000 (2006).
29. Pitulescu, M.E. & Adams, R.H. Eph/ephrin molecules—a hub for signaling and endocytosis. *Genes Dev.* **24**, 2480–2492 (2010).
30. Zhuang, G., Hunter, S., Hwang, Y. & Chen, J. Regulation of EphA2 receptor endocytosis by SHIP2 lipid phosphatase via phosphatidylinositol 3-Kinase-dependent Rac1 activation. *J. Biol. Chem.* **282**, 2683–2694 (2007).
31. Hiramoto-Yamaki, N. *et al.* Ephexin4 and EphA2 mediate cell migration through a RhoG-dependent mechanism. *J. Cell Biol.* **190**, 461–477 (2010).
32. Macrae, M. *et al.* A conditional feedback loop regulates Ras activity through EphA2. *Cancer Cell* **8**, 111–118 (2005).
33. Himanen, J.P. *et al.* Architecture of Eph receptor clusters. *Proc. Natl. Acad. Sci. USA* **107**, 10860–10865 (2010).
34. Seiradake, E., Harlos, K., Sutton, G., Aricescu, A.R. & Jones, E.Y. An extracellular steric seeding mechanism for Eph-ephrin signaling platform assembly. *Nat. Struct. Mol. Biol.* **17**, 398–402 (2010).
35. Wimmer-Kleikamp, S.H., Janes, P.W., Squire, A., Bastiaens, P.I.H. & Lackmann, M. Recruitment of Eph receptors into signaling clusters does not require ephrin contact. *J. Cell Biol.* **164**, 661–666 (2004).

ONLINE METHODS

p7560 Scaffold ssDNA preparation. From a single colony of *Escherichia coli* JM109 that was cultured overnight in 25 ml lysogeny broth (LB), 3 ml were diluted in 250 ml of 2xYT medium with 5 mM $MgCl_2$ and placed in a 37 °C shaker. When the optical density at 600 nm (OD_{600}) reached 0.5, p7560 phages were added at a multiplicity of infection (MOI) of 1, and incubation with shaking continued for an additional 5 h. The culture was transferred to a 250-ml centrifuge bottle and was centrifuged at 4,000*g* for 30 min, and the supernatant was centrifuged again at 4,000*g* for 20 min. 10 g PEG and 7.5 g NaCl (VWR international) were added to the supernatant containing p7560 phages, which was then incubated on ice for 30 min and centrifuged at 10,000*g* for 40 min. Next, the supernatant was removed, the pellet was resuspended in 10 ml of 10 mM Tris (pH 8.5, VWR International) and transferred to a 70-ml centrifuge bottle. 10 ml of a solution with 0.2 M NaOH (VWR), 1% SDS, was added, mixed gently by inversion and incubated at room temperature for 3 min. Then 7.5 ml of 3 M KOAc, pH 5.5, was added, gently mixed by swirling and incubated on ice for 10 min. The mixture was centrifuged at 16,500*g* for 30 min. The supernatant containing ssDNA was poured into fresh centrifuge bottles, and 50 ml 99.5% EtOH was added, mixed gently by inversion and incubated on ice for 30 min. The solution was centrifuged at 16,500*g* for 30 min. After the supernatant was decanted, the pellet was washed with 75% EtOH and air dried at room temperature for 15 min. Finally, the pellet was resuspended in 10 mM Tris, pH 8.5, and the concentration and quality were characterized by UV-Vis (NanoDrop, Thermo Scientific) and a 1.5% agarose gel, respectively.

Staple oligonucleotides preparation. Oligonucleotides (**Supplementary Table 1**) were purchased from Bioneer in 96-well plates. The staples in each well were diluted to a final concentration of 100 µM. Staples were mixed according to the method described in **Supplementary Figure 3**. The final concentration of the staples was adjusted to 200 nM each.

Ligand conjugation. *Step 1: 4FB modification of 3′ amino–modified oligonucleotide.* A pellet of 46 nmol of 3′ amino–modified oligonucleotide (Bioneer) was dissolved in 460 µl reaction buffer and washed with the same buffer three times in a Vivaspin 5K MWCO spin filter (centrifuged at 15,000*g*, 12 min, room temperature, Sartorius) and concentrated to 23 µl (2 mM of the oligonucleotide concentration). To this solution, 12.5 µl of 0.172 M Sulfo-S-4FB (Solulink) in DMF were added and incubated for 1 h at room temperature with occasional mixing. This procedure was repeated once. The reaction mixture was diluted with conjugation buffer (PBS, pH 6.0) and transferred to a Vivaspin 5K MWCO spin filter (prewetted with conjugation buffer) and washed with the same buffer seven times (centrifugation at 15,000*g*, 12 min, room temperature) and concentrated to 20 µl. The 4FB-modified oligonucleotide was then stored at 4 °C until further usage.

Step 2: HyNic modification of ligand and conjugation of modified ligand with modified oligonucleotide. 200 µg of lyophilized ephrin-A5-Fc (recombinant human ephrin-A5-Fc chimera, R&D Systems) was dissolved in 200 µl PBS, pH 7.4, and split to two 100-µl fractions, which were processed identically. 100 µl of ligand solution was buffer exchanged to PBS, pH 7.4, with Zeba Spin desalting columns, 7K MWCO (Thermo Fisher Scientific). 2 µl of 7.3 µM Sulfo-S-HyNic (Solulink) in DMF was added and incubated at room temperature for 2 h with occasional mixing. The ligand solution was buffer exchanged to PBS, pH 6.0, with Zeba Spin desalting columns, 7K MWCO, and 10 µl of the 4FB-modified oligonucleotide (ca. 10 eq.) was added and incubated at room temperature with occasional mixing. Upon completion, the ligand conjugate solution was diluted with PBS, pH 7.4, to 450 µl, transferred to an Amicon Ultrafiltration Unit, 50K MWCO (Millipore), and washed four times with PBS, pH 7.4. After the final wash, the volume was adjusted to 100 µl. To evaluate the efficiency of conjugation of ephrin-A5 to DNA, we measured absorption of light at 350 nm, giving an estimate of the ligand-to-oligonucleotide ratio. By carefully controlling of the conjugation chemistry, we were able to limit the average number of oligonucleotides conjugated to each ligand between 0.9 and 1.3.

Step 3: Rhodamine conjugation to oligonucleotide modified ligand. Rhodamine-NHS (Invitrogen) dissolved in DMF was added to the oligonucleotide-modified ligand in 100-fold molar excess and incubated at room temperature overnight. The excess rhodamine was removed with Zeba Spin desalting columns, 7K MWCO, pre-equilibrated with PBS, pH 7.4. The rhodamine conjugates were hybridized to nanocalipers and characterized as described in **Supplementary Figure 7**.

Ephrin-A5 nanocaliper production. The standard folding conditions used in this study were as follows: 20 nM ssDNA scaffold, 100 nM per staple, 13 mM $MgCl_2$, 5 mM Tris, pH 8.5, and 1 mM EDTA. Folding was carried out by rapid heat denaturation followed by slow cooling from 80 °C to 60 °C over 20 min, then from 60 °C to 24 °C for 14 h. Removal of excess staples or ligand conjugate was done by washing (repetitive concentration and dilution) the nanocalipers with PBS, pH 7.4, 10 mM $MgCl_2$ in 100-kDa MWCO 0.5-ml Amicon centrifugal filters (Millipore). Samples were diluted to 450 µl and transferred to a prewetted centrifugal filter and centrifuged at 14,000*g*, 15 °C, for 2 min, and then diluted again to 450 µl, mixed well and centrifuged again under the same conditions. The volume was adjusted with PBS, pH 7.4, 10 mM $MgCl_2$ to a nanocaliper concentration of 20 nM, and the sample was collected via centrifugation at 1,000*g* for 2 min. To remove excess staples, we washed the nanocalipers five times.

The ligand conjugates were added with a twofold excess to each protruding site on the nanocalipers and incubated in the PCR machine with a temperature ramp starting from 1 h at 37 °C followed by 14 h at 22 °C, and immediately after incubation the nanocalipers were stored at 4 °C. Removal of the excess conjugates was carried out by passing the samples consecutively through two Sepharose 6B (Sigma-Aldrich) loaded spin columns (Thermo Scientific; the first column was loaded with 400 µl and the second column loaded with 260 µl resin) and spun at 15 °C, 800*g*, for 3 min. The final concentration of the nanocalipers was adjusted to 20 nM by UV-Vis A260 measurement (default extinction coefficient for dsDNA in NanoDrop) of NC-empty as standard, and the ephrin-A5 nanocaliper concentration was calculated according to the gel band intensity ratio when compared to the standard (**Supplementary Fig. 8**).

Agarose gels for characterization of the ephrin-A5 nanocalipers. We prepared 2% agarose gels with 0.5× TBE supplemented

with 11 mM $MgCl_2$ (Sigma-Aldrich) and 0.5 mg/ml ethidium bromide (Sigma-Aldrich). We typically loaded 4 µl of 20 nM suspensions of nanostructures in each lane and ran the gels in 0.5× TBE with 11 mM $MgCl_2$ at 70 V for 4 h, cooled in an ice-water bath. We imaged the gels using a UV gel imaging system fitted with a digital camera (Uvipro Silver, Uvitec) and analyzed the images with ImageJ (NIH), MultiGauge (Fujifilm) and GelBandFitter[36].

Surface plasmon resonance (SPR). The extracellular domain of the human EphA2 receptor (recombinant human EphA2 CF, R&D Systems) was dissolved in 10 mM sodium acetate buffer, pH 4.5, and immobilized on a CM3 chip (GE Healthcare) according to manufacturer instructions. Ephrin-A5-Fc and Ephrin-A5-Fc oligonucleotide conjugate samples were diluted to concentrations ranging from 12 nM to 120 nM in PBS, pH 7.4, supplemented with 10 mM $MgCl_2$. Ephrin-A5 nanocaliper samples were diluted in PBS supplemented with 10 mM $MgCl_2$ to a final concentration ranging from 6 nM to 24 nM, and the binding was measured by BIAcore 2000 (GE Healthcare). The flow rate of the samples was adjusted to 5 µl/min, and a total amount of 35 µl was injected. Sensorgram data were processed with BIAevaluation 3.2 software (GE Healthcare).

EphA2 pulldown experiment. DNA nanocalipers were designed for pulldown experiments containing anchoring sites for the poly(A)-linked magnetic Dynabeads (Life Technologies) and sites with extra toehold sequences for elution of ephrin-A5–EphA2 complexes from the nanocalipers. The control nanocalipers with zero, one, two and three pairs of sites as well as NC100 and NC40 were folded in 13 mM Mg^{2+} folding buffer (5 mM Tris, 1 mM EDTA, pH 8.5). The excess of staples was washed away with Millipore Amicon 100K spin columns. Ephrin-A5 oligonucleotide conjugates were bound to structures by incubation in a thermal cycler on a 15-h-long thermal program from 37 °C to 4 °C. Ephrin-A5 nanocalipers were purified with spin column–based size-exclusion purification with Sepharose 6B beads. After the purification, the concentration of nanocalipers was measured with NanoDrop and was adjusted to 15 nM. 90 µl of 15 nM ephrin-A5 nanocaliper solution were incubated with magnetic Dynabeads overnight at 4 °C. Unbound nanocalipers were removed by washing with 10 mM Mg^{2+} folding buffer. After washing, the bound ephrin-A5 nanocalipers were incubated with 50 µl of 1 µM of EphA2 for 3 h at room temperature. The unbound fraction of EphA2 was removed by washing with 10 mM Mg^{2+} folding buffer. After washing, the ephrin-A5–EphA2 complexes were eluted from the bound nanocalipers by incubation of the nanocalipers with 40 µl of 1 µM of invading complementary oligonucleotide solution (10 mM Mg^{2+} folding buffer) overnight at 37 °C. Eluted samples were run under denaturing conditions (0.1% SDS) in a 10% PAGE gel (Bio-Rad, mini protean TGX). The gel was stained with the PlusOne Silver Staining Kit (GE Healthcare) and imaged with ChemiDoc XRS gel imager (Bio-Rad).

Western blotting. Eluted samples where run under nondenaturing conditions in a 10% PAGE gel (Bio-Rad, mini protean TGX) and transferred to a PVDF membrane (GE, Amersham Hybond). The membrane was incubated with goat anti-EphA2 antibodies (R&D systems, AF3035) (1:2,000 diluted in TBST with 1% milk powder) overnight at 4 °C. After washing, the membrane was incubated with HRP-conjugated rabbit anti-goat IgG (Dako, P0449) (1:2,000 diluted in TBST with 1% milk powder) for 1 h at room temperature. Chemiluminescent reagent (GE, Amersham ECL prime) was applied, and the membrane was imaged with ChemiDoc MP gel imager (Bio-Rad).

Transmission electron microscopy (TEM). We spotted 2 µl of the purified nanocaliper suspensions on glow-discharged, carbon-coated Formvar grids (Electron Microscopy Sciences), incubated for 20 s, blotted off with filter paper, and then stained with 2% (w/v) aqueous uranyl-formate solution followed by a final blot with filter paper. We performed TEM analysis using a FEI Morgagni 268(D) transmission electron microscope at 100 kV with nominal magnifications between 28,000× and 44,000×. Images were recorded digitally using the Advanced Microscopy Techniques Image Capture Engine 5.42.

Cell culture. MDA-MB-231 cells (generously provided by the lab of U. Lendahl, Karolinska Institutet, purchased from ATCC, free of mycoplasma (these cells were not recently authenticated)), were cultured in Dulbecco's modified Eagle medium supplemented with 10% fetal bovine serum and 1% penicillin/streptomycin. For immunocytochemistry and PLA experiments, cells were cultured on 16-well glass slides (Thermo Fisher Scientific) or on micropatterned glass slides (CYTOO) to obtain single cells of uniform size and shape, which are unable to form cell-cell contacts. The micropatterns consisted of disc-shaped fibronectin patterns approximately 30 µm in diameter and spaced 80 µm apart. Cells were detached using warm TrypLE Express (Gibco) and seeded onto the patterns at 60,000 cells/ml. The cells were allowed to attach for 1 h before the unattached cells were washed off.

Eph receptor stimulation. Prior to EphA2 receptor stimulation, the cells were serum starved for 1 h. Ephrin-A5-Fc homodimers (recombinant human ephrin-A5-Fc chimera, R&D Systems, cat. no. 374-EA-200) were preclustered with IgG antibodies (polyclonal AffiniPure Goat Anti-Human IgG, Jackson ImmunoResearch Laboratories Inc., cat no. 109-005-008) at a mass ratio of 1:10 for 15 min at room temperature, which is a commonly used method to cluster ephrin ligands, hereafter referred to as IgG-clustered ephrin-A5. Cells were treated for 15 min at 37 °C with either 5 µg/ml IgG or 0.5 µg/ml of ephrin-A5 monomer (Creative Biomart), ephrin-A5 dimer or IgG-clustered ephrin-A5. For experiments with nanocalipers, cells were treated with 10 nM of ephrin-A5-Fc, which corresponds to 0.5 µg/ml, conjugated to DNA nanocalipers (NC0, NC100, NC40 and NC-sat) or empty nanocalipers (NC-empty) as controls.

Immunocytochemistry. Cells were serum starved for 1 h before stimulation with IgG, ephrin-A5 monomer, ephrin-A5 dimer, IgG-clustered ephrin-A5, NC-empty, NC0, NC100 and NC40 for 120 min at 37 °C. For dynamin inhibition, Dyngo-4a (Abcam) was added to the serum-free medium at 30 µM, and DMSO was used as control. After EphA2 stimulation, cells were rinsed once with PBS and fixed for 20 min in 10% formalin at room temperature. The cells were washed three times with PBS/0.1% Triton X-100 and stained overnight at 4 °C in PBS/0.1% Triton X-100/1% BSA with the following antibodies: anti-EphA2 (1:500, Santa Cruz Biotechnology,

doi:10.1038/nmeth.3025

cat. no. sc-924) and anti-EEA1 (1:1,000, BD Biosciences, cat. no. 610457). The samples were washed six times with PBS/0.1% Triton X-100 and then treated with the species-specific secondary antibodies Alexa Fluor 488 (1:500, Invitrogen, cat. no. A21206) and Cy3-conjugated AffiniPure IgG (1:450, Jackson ImmunoResearch Laboratories, cat. no. 715-165-150) diluted in PBS/0.1% Triton X-100/1% BSA for 1 h in the dark. Finally, samples were washed with PBS and mounted in Vectashield with 4′,6-diamidino-2-phenylindole (DAPI). Images were acquired using a Zeiss LSM700 CLSM confocal microscope.

***In situ* proximity ligation assay (PLA).** Unless stated otherwise, all reagents for the PLA were from Sigma-Aldrich. Upon EphA2 stimulation, cells were washed once with warm PBS and fixed in 10% formalin for 20 min at room temperature. The cells were washed three times for 5 min each in PBS with gentle agitation, followed by three washes with PBS/0.1% Triton X-100 for 10 min each and three washes with TBS-0.05% Tween 20 for 5 min. The samples were incubated with Duolink II Blocking Solution in a humidity chamber for 1 h at 37 °C. For detection of EphA2 receptor phosphorylation, the following antibodies and dilutions were used: anti-phosphotyrosine (1:1,200, Abcam, cat. no. ab9319) and anti-EphA2 (clone D7, specific for intracellular domain[37], 1:1,500, Millipore, cat. no. 05-480). Antibodies were diluted in the Duolink II Antibody Diluent (1×) and incubated overnight at 4 °C in a humidity chamber. The next day, the cells were washed three times for 10 min with 1× Duolink II Wash Buffer A. The two PLA probes, Duolink II anti-Mouse PLUS and Duolink II anti-Rabbit MINUS, were diluted 1:80 in Antibody Diluent, and samples were incubated for 60 min in a humidity chamber at 37 °C. All samples were washed three times for 10 min in 1× Duolink II Wash Buffer A. The Duolink II Ligation stock (5×) was diluted five times in water, and the ligase was diluted 1:80 in the ligation mix. Samples were incubated in the ligase-ligation solution for 30 min at 37 °C in a humidity chamber. The slides were washed twice for 2 min in 1× Duolink II Wash Buffer A. The Duolink II Amplification stock (5×) was diluted five times in water and used to dilute the polymerase 1:160. The samples were incubated in amplification-polymerase solution in a humidity chamber for 60 min at 37 °C. Finally, the samples were washed twice for 10 min with 1× Duolink II Wash Buffer B and once for 5 min with PBS. The cells were stained with Alexa Fluor 488–phalloidin (1:100, Invitrogen) and mounted with Vectashield with DAPI. Images for PLA signal analysis were acquired using Zeiss Cell Observer fluorescent microscope. *z*-stack images with 40× magnification were acquired in "Start/stop mode" (at least 20 stacks with 3-µm step size) for at least 20 cells per condition. The number of biological repeats was: $n = 7$ for IgG, ephrin-A5 dimer and IgG-clustered ephrin-A5; $n = 5$ for ephrin-A5 monomer (two biological replicates were excluded for the monomer because the results were anomalous and we confirmed by native gel electrophoresis the presence of clustered monomers in these repeats); $n = 6$ for NC-empty, NC100 and NC40; and $n = 4$ for NC0 (all performed experiments were included). Maximal-intensity projection of the *z* stacks was performed using the open-source cell image analysis software CellProfiler (http://www.cellprofiler.org/). Fluorescence images for **Figure 3a**,**c** were acquired with a Zeiss LSM700 confocal microscope. We quantified the PLA signals in **Figure 3b**,**d** by selecting all single cells for every experimental group on the basis of the DAPI images (without seeing the PLA signal). The PLA signals were quantified with BlobFinder using batch processing, and all measurements were included in the analysis.

Flow cytometry. To verify that the ephrin-A5 nanocalipers bound MDA-MB-231 cells, we performed flow cytometry on cells stimulated with IgG-clustered ephrin-A5 and NC-sat. Empty nanotubes (NC-empty) and IgG alone were used as controls. Specifically, the MDA-MB-231 cells were collected with a cell scraper and kept on ice until treated. DyLight 488–conjugated AffiniPure Donkey Anti-Human IgG (Jackson ImmunoResearch Laboratories, cat. no. 709-485-149) was used to precluster ephrin-A5-Fc for 15 min (20 µg/ml IgG and 2 µg/ml ephrin-A5 dimer). Alternatively, DyLight 488-conjugated AffiniPure Donkey Anti-Human IgG was added to the cell culture medium 15 min after the start of stimulation with NC-sat and NC-empty. Flow cytometry was performed two times per condition on FACSCanto II, and the percentage of FITC-positive cells was measured and analyzed using FACSDiva software (BD Biosciences).

Immunoprecipitation. MDA-MB-231 cells were seeded at 12,000 cells/cm^2 in six-well plates and were stimulated with ephrin-A5 for 15 min as previously described. Cells were lysed in 500 µl of modified RIPA buffer (50 mM Tris, pH 7.4, 150 mM NaCl, 10% glycerol, 1% NP-40, 0.5% sodium deoxycholate, 1 mM EDTA, 1 mM sodium vanadate, 1 mM NaF, phosphatase inhibitor cocktail (Sigma-Aldrich) and protease inhibitor cocktail (Roche)). The lysed material was precleared by centrifugation at 14,000*g* for 10 min in 4 °C. For the immunoprecipitation experiments, 250 µl of precleared lysate were incubated with 1.25 µg of mouse monoclonal anti-EphA2 antibody (Millipore, cat. no. 05-480) for 18 h in end-over-end rotation at 4 °C. Next, 25 µl of an approximately 50% slurry of Sepharose-G beads (GE Healthcare) were added and incubated for an additional 4 h. The beads were collected by centrifugation at 9,000 r.p.m. on a benchtop centrifuge for 30 s and washed three times in 1 ml of ice-cold lysis buffer. After the final wash, the beads were boiled at 95 °C for 5 min in Laemmli/SDS loading buffer with 5% β-mercaptoethanol and separated in an SDS-page gel (Bio-Rad). Proteins on the gel were transferred to a PVDF membrane (Immobilon-P, Millipore) by wet transfer and blocked by 5% BSA in PBS overnight. The membrane was incubated with an anti-phosphotyrosine antibody (1:500, Abcam, cat. no. ab9319) overnight, washed extensively in TBST buffer, and detected with anti-rabbit HRP (1:20,000 dilution, GE Healthcare, cat. no. RPN4301) and ECL detection reagents (Millipore, cat. no. WBKLS00500). The membranes were stripped at 55 °C in a buffer containing 62.5 mM Tris-HCl, pH 6.8, 2% SDS and 7 µl/ml β-mercaptoethanol, blocked with BSA (5%) in TBS and reprobed with anti-EphA2 antibody (1:1,000, Santa Cruz, cat. no. sc-924) followed by anti-rabbit HRP (1:20,000, GE Healthcare) and detected with ECL detection reagents (Millipore).

Cell invasion assay. We performed a cell invasion assay to study the effects of EphA2 receptor stimulation on MDA-MB-231 cell migration through an extracellular matrix (ECM). The assay was performed in two biological repeats using ECMatrix precoated cell culture inserts with 8-µm pores (Merck Millipore). To rehydrate the ECM layer, we kept the inserts in serum-free medium

for 2 h at room temperature before cell seeding. Cells were collected with a cell scraper and treated for 15 min at 37 °C with 20 µg/ml of IgG; 2 µg/ml of ephrin-A5 monomer, ephrin-A5 dimer or IgG-clustered ephrin-A5 (preclustered with IgG at a mass ratio of 1:10 for 15 min at room temperature); or 10 nM of ephrin-A5-Fc conjugated to DNA nanocalipers (NC100 or NC40) or empty nanocalipers (NC-empty) as control. 40,000 cells were seeded in each insert in 200 µl serum-free medium, and the lower chamber was filled with 500 µl medium containing serum. After 24 h of culture, cells were washed with PBS, fixed for 2 min in 10% formalin at room temperature and permeabilized for 10 min with 100% methanol. Cells were stained using the cell stain supplied by the manufacturer as well as DAPI, and non-invading cells were gently removed from the interior of the inserts using a cotton-tipped swab. Images were acquired using a fluorescent Zeiss Axioscope2 microscope, and the total number of cells in seven 5× images was counted for each condition.

Statistical analysis. For multiple-comparison analysis in **Figure 3b**,**d**, we performed one-way ANOVA followed by Tukey post tests. Using Prism software (GraphPad), we performed the D'Agostino-Pearson omnibus normality test, which showed that each group of data followed a normal distribution. Further, Bartlett's test for equal variances showed that the variances were similar between the groups. The number of biological repeats was chosen on the basis of preliminary data of PLA for EphA2 phosphorylation of cells on micropatterns, and we did not perform power calculations before the experiment. In **Figure 4e**, we performed Student's *t*-test; the sample size, $n = 3$, was too small to determine normality, and the *F*-test showed that the variances were similar in the different groups. The data in **Figure 4e** are two biological replicates and the sample size was too small to determine normality or equal variances.

36. Mitov, M.I., Greaser, M.L. & Campbell, K.S. GelBandFitter—a computer program for analysis of closely spaced electrophoretic and immunoblotted bands. *Electrophoresis* **30**, 848–851 (2009).
37. Coffman, K.T. *et al.* Differential EphA2 epitope display on normal versus malignant cells. *Cancer Res.* **63**, 7907–7912 (2003).

doi:10.1038/nmeth.3025